Improving the antifouling property of poly(vinyl chloride) membranes by poly(vinyl chloride)-*g*-poly(methacrylic acid) as the additive

Li-Feng Fang, Ming-Yong Zhou, Na-Chuan Wang, Bao-Ku Zhu, Li-Ping Zhu

Department of Polymer Science and Engineering, Key Laboratory of Macromolecular Synthesis and Functionalization (Ministry of Education), Engineering Research Center of Membrane and Water Treatment (Ministry of Education), Zhejiang University, Hangzhou 310027, People's Republic of China
Correspondence to: B.-K. Zhu (E-mail: zhubk@zju.edu.cn)

ABSTRACT: To improve the antifouling property of poly(vinyl chloride) (PVC) membranes, a series of poly(methacrylic acid) grafted PVC copolymers (PVC-*g*-PMAA) with different grafting degree were synthesized via one-step atom transfer radical polymerization process utilizing the labile chlorines on PVC backbones followed by one-step hydrolysis reaction. PVC/PVC-*g*-PMAA blend membranes with different grafting degree and copolymer content were prepared by nonsolvent induced phase separation method. The surface chemical composition, surface charge, membrane structures, wettability, permeability, separation performances and the fouling resistance of blend membranes were carefully investigated. The results indicated that the PMAA chains were segregated towards the surface and the membranes were endowed with negative charge. The hydrophilicity and permeability of the blend membranes were obviously improved. Furthermore, the antifouling ability especially at neutral or alkaline environments was also significantly increased. © 2015 Wiley Periodicals, Inc. J. Appl. Polym. Sci. **2015**, *132*, 42745.

INTRODUCTION

Poly(vinyl chloride) (PVC) is one of the most extensively used membrane materials for ultrafiltration and microfiltration due to its low cost, robust mechanical strength, excellent solvent resistance, etc.[1,2] However, the membranes tend to adsorb or deposit natural organic matter, colloids, and microorganisms during filtration process because of its intrinsic hydrophobicity. Usually, the hydrophilic modification of polymer membranes is one of the most effective ways to improve the fouling resistance property so as to achieve lower operation pressure, less physical and chemical cleaning and longer membrane life.[3–9]

Poly(methacrylic acid) (PMAA) and poly(acrylic acid) (PAA) are well known hydrophilic polymers used for membrane modification. Many investigators have published articles on the hydrophilic modification of membranes via grafting or blending either PMAA/PAA or other copolymers on to/into the membranes matrix.[10–16] Hester et al.[13,17] have prepared a comb-like PMAA grafted poly(vinylidene fluoride) via atom transfer radical polymerization (ATRP) followed by hydrolysis process. The PMAA chains were segregated to the surface of membrane and the hydrophilicity was remarkably improved. Similarly to reduce

the hydrophobicity of membranes, Hidzir et al.[11] have grafted PAA chains on to poly(tetrafluoroethylene) membranes via radiation-induced grafting copolymer. Recently, Saffar et al.[10] have prepared hydrophilic polypropylene (PP) membranes by blending commercial acrylic acid grafted PP (PP-*g*-AA) via melt extrusion. Therefore, introducing PMAA or PAA into polymer membranes could obviously promote their hydrophilicity.

Considering the effectiveness of PMAA or PAA, a few methods have been proposed by various research groups to introduce them into PVC membranes. Muth et al.[18] have introduced the PMAA chains into PVC by supercritical impregnation in which, there was no formation of chemical bonds between PMAA and PVC matrix. Liu et al.[19,20] have grafted PAA chains on to cross-linked PVC particles via surface-initiated ATRP and hydrolysis. However, their work mainly focused on the adsorption of heavy metal ions utilizing the chelate ability of carboxylic groups. In our group,[21] a series of poly(methyl methacrylate-*b*-methacrylic acid) (PMMA-*b*-PMAA) have been synthesized via two-step ATRP process and one-step hydrolysis. These PVC/PMMA-*b*-PMAA blend membranes were endowed with improved hydrophilicity and enhanced antifouling property. Though PMMA-*b*-PMAA was proven to be a useful amphipilic additive for

Additional Supporting Information may be found in the online version of this article.
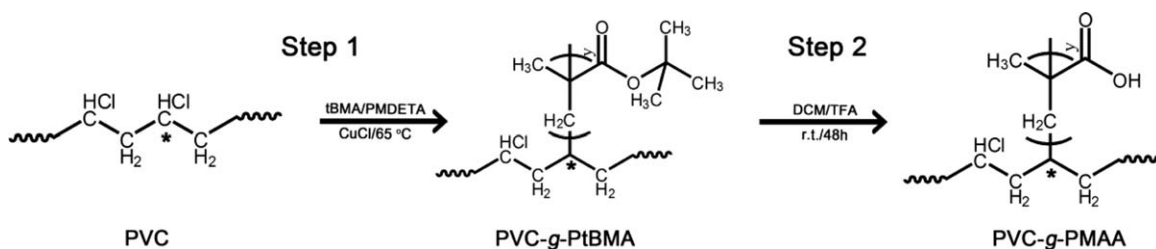
Figure 1. Synthesis of PVC-g-PMAA (step 1: grafting tBMA on to PVC via ATRP process; step 2: hydrolysis of PVC-g-PtBMA; the star (*) represents the tertiary chlorines and internal allylic chlorines in PVC backbones).

membrane modification, it needed two-step ATRP reaction and one-step hydrolysis reaction which was a relatively complicated synthesis procedure and difficult for producing such an additive in large scale.

In this work, the authors have provided a relatively facile way to prepare PMAA grafted PVC copolymer (PVC-g-PMAA) via one-step ATRP reaction by initiating the labile chlorines on PVC backbones[22–25] followed by one-step hydrolysis reaction. Due to the reactive protons in methacrylic acid (MAA), *tert*-butyl methacrylate (tBMA) was employed as the transitional monomer during ATRP process. The composition of the copolymer was changed by regulating the reaction time. PVC/PVC-g-PMAA blend membranes were fabricated by nonsolvent induced phase separation (NIPS) method. The surface chemical composition, surface charge, wettability, permeability and separation performance were carefully investigated. Since the PMAA chains are highly responsive to the environment,[17,26,27] the protein adsorption resistance and antifouling ability at different pH environment were also studied.

EXPERIMENTAL

Materials

PVC ($M_w = 81,000$ g mol^{-1}) was purchased from Qilu Petrochemical and was dried thoroughly before use. *Tert*-butyl methacrylate (tBMA) was supplied by Aladdin Chemical, which was passed through a column of aluminum oxide to remove the inhibitor before use. CuCl was obtained from Sinopharm Chemical Reagent, which was washed with acetic acid and ethanol several times and then dried under low pressure before use. Pentamethyldiethylenetriamine (PMDETA) was supplied by Sigma-Aldrich and used as received. Bovine serum albumin (BSA) was bought from Sangon Biotech. *N*-methyl pyrrolidone (NMP), tetrahydrofuran (THF), trifluoroacetic acid (TFA),

dichloromethane (DCM), and other regular reagents were bought from Sinopharm Chemical Reagent and used as received without further purification.

Synthesis and Characterization of PVC-g-PMAA

The synthesis procedure for PVC-g-PMAA mainly involves two steps as shown in Figure 1. In the first step, tBMA is grafted on to PVC via ATRP process and the second step involves the hydrolysis of PVC-g-PtBMA. The detailed procedure during step 1 is as follows. Initially, 2.0 g of PVC resin was dissolved in NMP in a three-necked flask and then 3.0 g (0.021 mol) of tBMA, 54.4 mg (0.031 mmol) of PMDETA and 54.4 mg (0.31 mmol) of CuCl were introduced into the flask. This mixture was stirred and bubbled continuously with dry nitrogen for 30 min at 0°C. Then the reaction was carried at 65°C for a predetermined time. After polymerization, the solution was cooled and diluted with THF and then it was passed through a silica column to remove copper. The filtrate containing graft polymer was precipitated in the mixture of ethanol/water (v/v = 1/1). Then the graft copolymer was further purified by dissolution and precipitation for three cycles. Finally, the resultant product (PVC-g-PtBMA) was dried in vacuum oven at 40°C for 24 h. PVC-g-PtBMA was then hydrolyzed in TFA/DCM, where TFA acts as the catalyst. The detailed procedure for step 2 is described as follows. In a container, 2.0 g of PVC-g-PtBMA was dispersed in 50 mL of DCM and then TFA was added to it in excess. The hydrolysis reaction was carried out at room temperature for 48 h. After that, the resultant crude product was dried by distillation and the residue was rinsed with ethanol for several times, from which PVC-g-PMAA was obtained. PVC-g-PtBMA acquired after different reaction time (1.0, 2.0, 4.0, and 6.0 h) are denoted by PtBMA1.0, PtBMA2.0, PtBMA4.0, and PtBMA6.0, respectively. Corresponding PVC-g-PMAA copolymer are labeled according to the PMAA grafting degree (i.e.,

Table I. Compositions of PVC and PVC/PVC-g-PMAA Blend Membranes

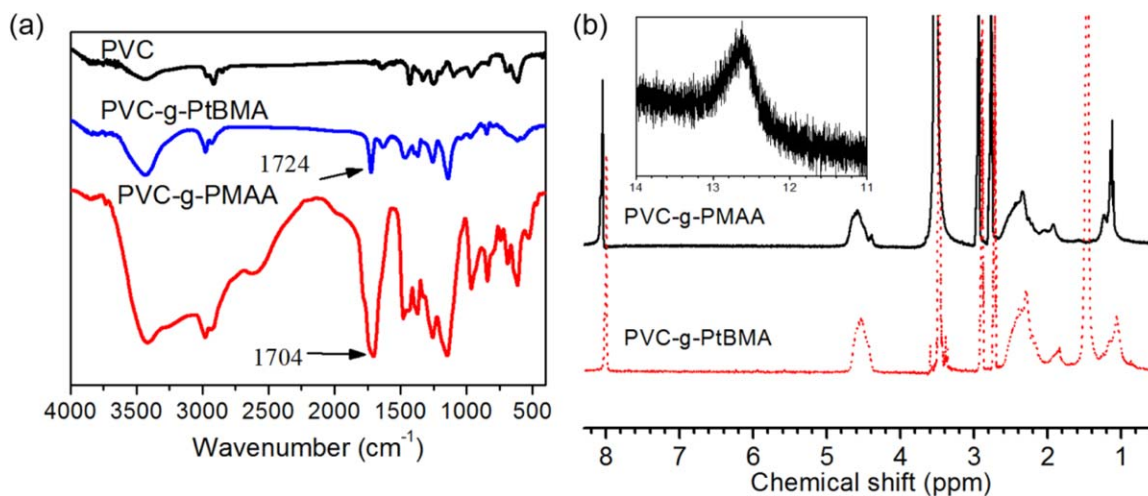| Membrane ID	PVC g^{-1}	Type of copolymer	Copolymer g^{-1}	DMAc g^{-1}
PVC	17	–	–	83.0
M-PMAA20.3%	13.6	PMAA20.3%	3.4	83.0
M-PMAA27.9%	13.6	PMAA27.9%	3.4	83.0
M-PMAA40.6%	13.6	PMAA40.6%	3.4	83.0
M-PMAA51.7%	13.6	PMAA51.7%	3.4	83.0
M-PMAA27.9–5%	16.2	PMAA27.9%	0.85	83.0
M-PMAA27.9–10%	15.3	PMAA27.9%	1.7	83.0

Figure 2. (a) Typical IR and (b) 1H NMR spectra of PVC, PVC-*g*-PtBMA (PtBMA4.0), and PVC-*g*-PMAA (PMAA40.6%). [Color figure can be viewed in the online issue, which is available at wileyonlinelibrary.com.]

PMAA20.3, PMAA27.9, PMAA40.6, and PMAA51.7%), respectively.

The infrared (IR) spectra of copolymer were obtained from a Bruker Vector 22 Fourier transform infrared spectrometer between the wavenumbers from 400 to 4000 cm^{-1}. The copolymer was dissolved in deuterated dimethyl formamide (DMF) to acquire the proton nuclear magnetic resonance (1H NMR) spectra using a Varian Unity Plus 300/54 NMR spectrometer at 40°C with $Si(CH_3)_4$ as the standard reference. The molecular weight and polydispersity index of copolymers were determined by gel permeation chromatography (GPC, Waters 510 HPLC pump/Waters Styragel columns/Waters410 differential refractometer) using DMF as an eluent.

Preparation and Characterization of Membranes

The PVC pure membrane and PVC/PVC-*g*-PMAA blend membranes were prepared via NIPS method. The compositions of the casting solutions are listed in Table I.

Attenuated total reflectance Fourier transform infrared (ATR-FTIR) spectra were collected using Nicolet NEXUS 6700 spectrometer (Thermo Fisher Scientific) from 400 to 4000 cm^{-1} with a scan rate of 4 cm^{-1} s^{-1}. X-ray photoelectron spectroscopy (XPS) data were obtained from PHI 5000C ESCA system with Mg Kα excitation radiation ($h\nu = 1253.6$ eV). The carboxylic group concentration on the surface of PVC/PVC-*g*-PMAA membrane was determined by toluidine blue O (TBO)

method.[28,29] The membrane structures were observed using scanning electron microscopy (SEM, Hitachi S-4800). The cross section was acquired after fracturing the membranes in liquid nitrogen. The surfaces and cross sections were sputtered with gold by ETD-200 sputter coater (Elaborate Technology Development) prior to the test.

The porosity ($P(\%)$) of the membrane was calculated according to the equation, $P(\%) = (m_2 - m_1)/(\rho V_1) \times 100$; where, m_1 and m_2 are the weights of dry and wetted (saturated adsorption of isopropanol) membranes, respectively, V_1 is the volume of the dry membrane and ρ is the density of isopropanol. Surface wettability of the membranes was characterized by water contact angle determination. The surface charge was determined on a Zeta potential electrokinetic analyzer (Anton Paar GmbH SurPASS, Austria) according to the Helmholtz–Smoluchowski equation[30,31] with 1 mmol L^{-1} KCl solution at room temperature. A series of zeta potential measurements were performed at different pH environments, where the pH of solution was changed from 2.5 to 10 by adding HCl and NaOH solution. The filtration performance was tested in a Millipore UF stirred cell (XFUF047) at room temperature. The water flux (J_w, L m^{-2} h^{-1}) of tested membrane was determined by measuring the volume (V_w) of permeate. The J_w is calculated by the equation, $J_w = V_w/(St)$, where, S and t are the effective filtration area ($S = 15$ cm^2) and testing time (h), respectively. In order to investigate the antifouling property of the membranes at various

Table II. M_n, PDI, and Chemical Compositions of PVC-*g*-PtBMA and PVC-*g*-PMAA

Product ID	M_n	PDI	tBMA %[a]	MAA %[b]	Grafting degree/%[a]
PVC	79,308	2.10	–	–	–
PtBMA1.0	107,371	2.11	25.1	16.9	20.3
PtBMA2.0	112,331	2.28	31.5	21.8	27.9
PtBMA4.0	123,362	2.39	40.1	28.9	40.6
PtBMA6.0	126,956	2.52	46.1	34.1	51.7

[a,b]Calculated according to 1H NMR results.
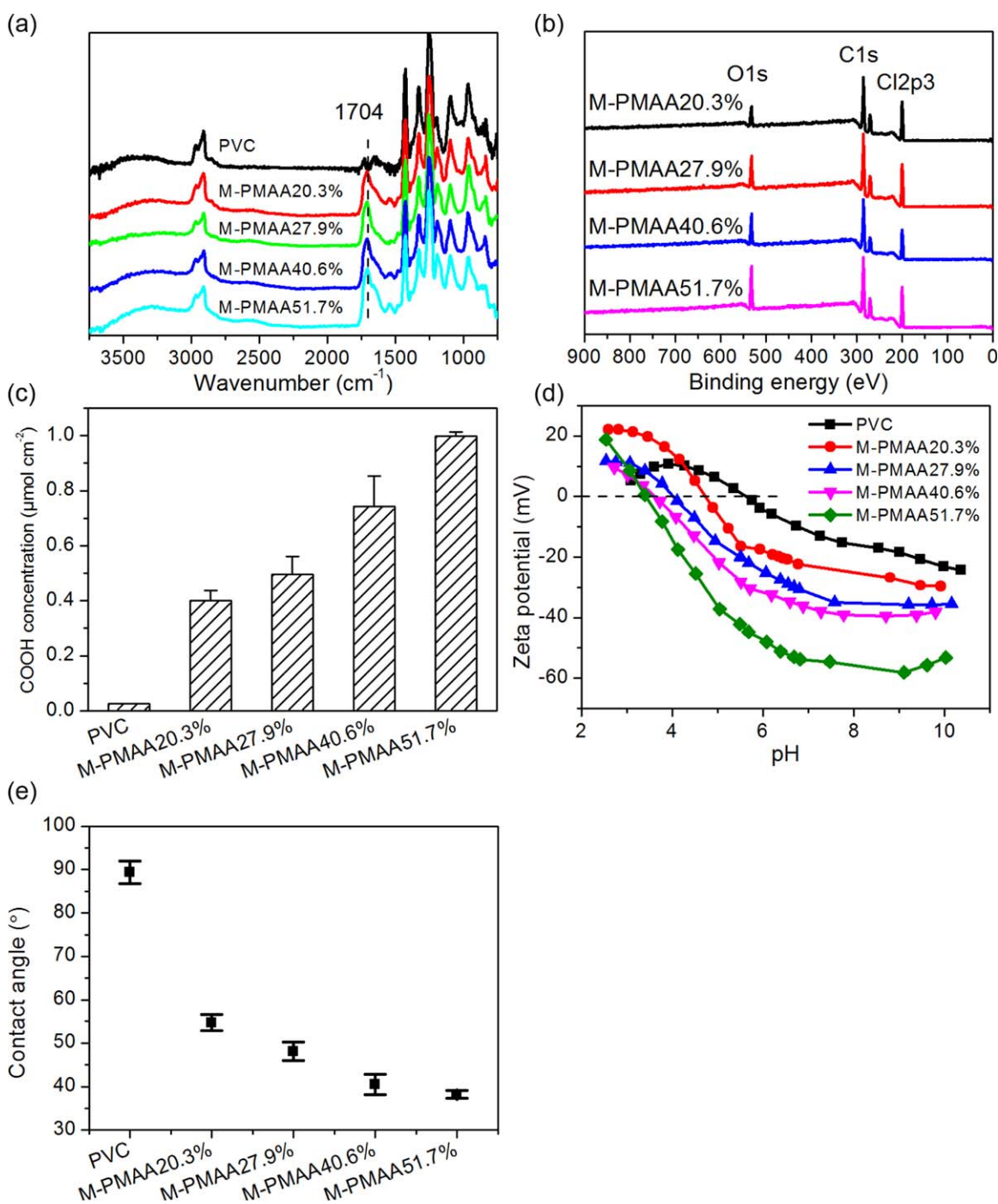[a]Presenting the PMAA grafting degree in PVC-*g*-PMAA.

Figure 3. (a) ATR-FTIR spectra, (b) XPS spectra, (c) surface COOH concentration, (d) Zeta potential plotted against pH, and (e) contact angles of PVC and PVC/PVC-g-PMAA blend membranes. [Color figure can be viewed in the online issue, which is available at wileyonlinelibrary.com.]

pH, the protein filtration experiment was carried out at different pH (3.0, 4.8, 7.4, and 11.0). At first, the flux (J_{w1}) of solution with a certain pH was measured for 1 h (0.1 MPa). Then BSA solution (0.1 g L^{-1}) with the determined pH was forced to passed through the membrane, and the final stable flux (J_p) was recorded after 1 h. The membranes were then rinsed with distilled water for 30 min to remove the adhered foulants on the surface. Finally, the flux (J_{w2}) of water with the initial pH was tested again. The BSA rejection was calculated by

$R(\%) = (1 - c^{\text{permeate}}/c^{\text{feed}}) \times 100$, where, c^{permeate} and c^{feed} are the concentrations of permeate and feed, respectively, which were determined by UV–vis spectrometer (HP 8453) at a wavenumber of 280 nm. The protein adsorption experiment was also performed to testify the antifouling property of the membranes. BSA was used as the model foulant. The procedure is as follows. The membrane was cut into a circular shape with 14 mm diameter using a hole punch. After preserved in ethanol/water (v/v = 1/1) for 10 min, the membrane was rinsed for 30 min by

Table III. Chemical Compositions of PVC/PVC-g-PMAA Blend (M-PMAA20.3, M-PMAA27.9, M-PMAA40.6, and M-PMAA51.7%) Membranes

Membrane ID	C mol^{-1} %	Cl mol^{-1} %	O mol^{-1} %	PMAA % in casting solution	PMAA % in near surface	Enrichment ratio[a]
M-PMAA20.3%	71.4	17.0	11.5	3.38	33.2	9.8
M-PMAA27.9%	68.1	16.4	15.5	4.36	39.6	9.0
M-PMAA40.6%	67.4	16.2	16.4	5.78	45.6	7.9
M-PMAA51.7%	66.3	14.1	19.6	6.82	49.0	7.2

[a] Enrichment ratio means the ratio of PMAA % in near surface and that in casting solution.

phosphate buffer solution (PBS) with different pH (3.0, 4.8, 7.4, and 11.0). Then the membrane was transferred to 2 mL of protein solution (0.5 g L^{-1}) and the solution was vibrated at 30°C for 8 h. The concentrations of BSA solution before and after adsorption were determined by UV–vis spectrometer.

RESULTS AND DISCUSSION

Synthesis of PVC-g-PMAA

Figure 2(a) shows the typical IR spectra of PVC, PVC-g-PtBMA, and PVC-g-PMAA. Compared to PVC, there is a characteristic peak at 1724 cm^{-1} in the spectrum of PVC-g-PtBMA, which is attributed to the stretching vibration of carbonyl (C=O) group in tBMA. This indicates the successful grafting of tBMA on to PVC. While in the PVC-g-PMAA spectrum, the characteristic band peak of C=O group shift towards the lower wavenumber, that is 1704 cm^{-1} represents C=O in protonated carboxylic acid.[32] Moreover, the broad peak in the range of 3000–3800 cm^{-1} belongs to the characteristic adsorption of hydroxyl group in carboxylic acid. These results primarily suggest that tBMA has been grafted on to PVC and PVC-g-PtBMA has turned into PVC-g-PMAA after the hydrolysis reaction.

PVC-g-PtBMA and PVC-g-PMAA were also confirmed by 1H NMR and the spectra are shown in Figure 2(b). Compared to PVC-g-PtBMA spectrum, the proton adsorption peak at 1.4 ppm (assigned to the proton on *tert*-butyl group) disappears in PVC-g-PMAA curve, which indicates that at least 95% of the tBMA repeated units have been hydrolyzed.[33] In addition, a proton adsorption peak at 12.6 ppm, which corresponds to the proton in carboxylic acid group is found in PVC-g-PMAA curve. Furthermore, the chemical composition of the PVC-g-PtBMA can be calculated from the ratio between the area of PVC (4.5 ppm, —CHCl—) and PtBMA (1.4 ppm, —C—CH$_3$) characteristic peaks. While for the compositions of PVC-g-PMAA copolymers, they were calculated according to the ratio between the area of PVC (4.5 ppm, —CHCl—) and PMAA (0.8–1.1 ppm, C—CH$_3$). The compositions of all copolymers are listed in Table II. The molecular weight (M_n) and polydispersity index (PDI) of PVC-g-PtBMA were confirmed by GPC (Table II and Figure SI, Supporting Information). All the graft products exhibit only one peak in the elution curve, which implies that the products are copolymers rather than blends. With increase in reaction time, the elution curve shift towards the higher molecular weight. All the above characterizations give a strong evidence for the successful grafting of MAA on to PVC backbones with only two-step process and the PMAA content in the copolymer could be regulated by adjusting the reaction time.

Effect of PMAA Grafting Degree in PVC-g-PMAA on the Structures and Performances of the Membranes

The surface chemical composition of blend membranes was determined by ATR-FTIR and XPS, and the results are shown in Figure 3. In Figure 3(a), there is a strong adsorption peak at 1704 cm^{-1} in the spectra of blend membranes indicating that the copolymer, PVC-g-PMAA has been introduced into the blend membranes. Moreover, with the increase of PMAA grafting degree in copolymers (from 20.3 to 51.7%), the intensity of adsorption peak at 1704 cm^{-1} increases, which primarily illustrates the increasing PMAA content in the surface of blend membranes. From the XPS survey spectra for blend membranes [Figure 3(b)], the signal corresponding to oxygen element (532.1 eV, O1s) can be observed. The oxygen content in the near surface (about 10 nm depth) increases with the PMAA content in the copolymers, which confirms the increase of PMAA content in the surface. The data of full elemental analysis are displayed in Table III. It can be noticed that the PMAA content in the near surface is much higher than that in casting solution, that is, there are about 8.8 times more PMAA chains in the near surface of M-PMAA20.3% than those in the casting solution. This obviously proves the surface segregation. Due to the enhanced interaction between PMAA chains and the coagulation bath, PMAA chains tend to migrate towards the interface between polymer membrane and coagulation bath during membrane formation process. Meanwhile, the blend membrane with high molecular weight copolymer displays the low enrichment ratio (the ratio of PMAA content in near surface and that in casting solution). This may be caused by worse mobility of the copolymer with longer grafting chains during phase separation.[12,34]

The concentration of carboxylic acid group (COOH) on the surface of PVC/PVC-g-PMAA blend membrane was measured by TBO method. In the alkaline solution, the TBO molecules with positive charge would be adsorbed by the negative carboxylic acid group on the membrane surface because of the electrostatic interaction.[28] After the saturated adsorption, the membrane was immersed in acid solution to elute TBO. The TBO concentration was then determined by UV–vis spectrometer at 633 nm from which the surface COOH concentration was calculated. Figure 3(c) displays the surface COOH concentration on the PVC and PVC/PVC-g-PMAA membranes. They are 0.40, 0.50, 0.74, and 1.00 μmol cm^{-2} for M-PMAA20.3, M-PMAA27.9, M-PMAA40.6, and M-PMAA51.7%, respectively. Apparently, the surface COOH concentration increases with the PMAA content in PVC-g-PMAA, which is in accordance with the ATR-FTIR and XPS results.
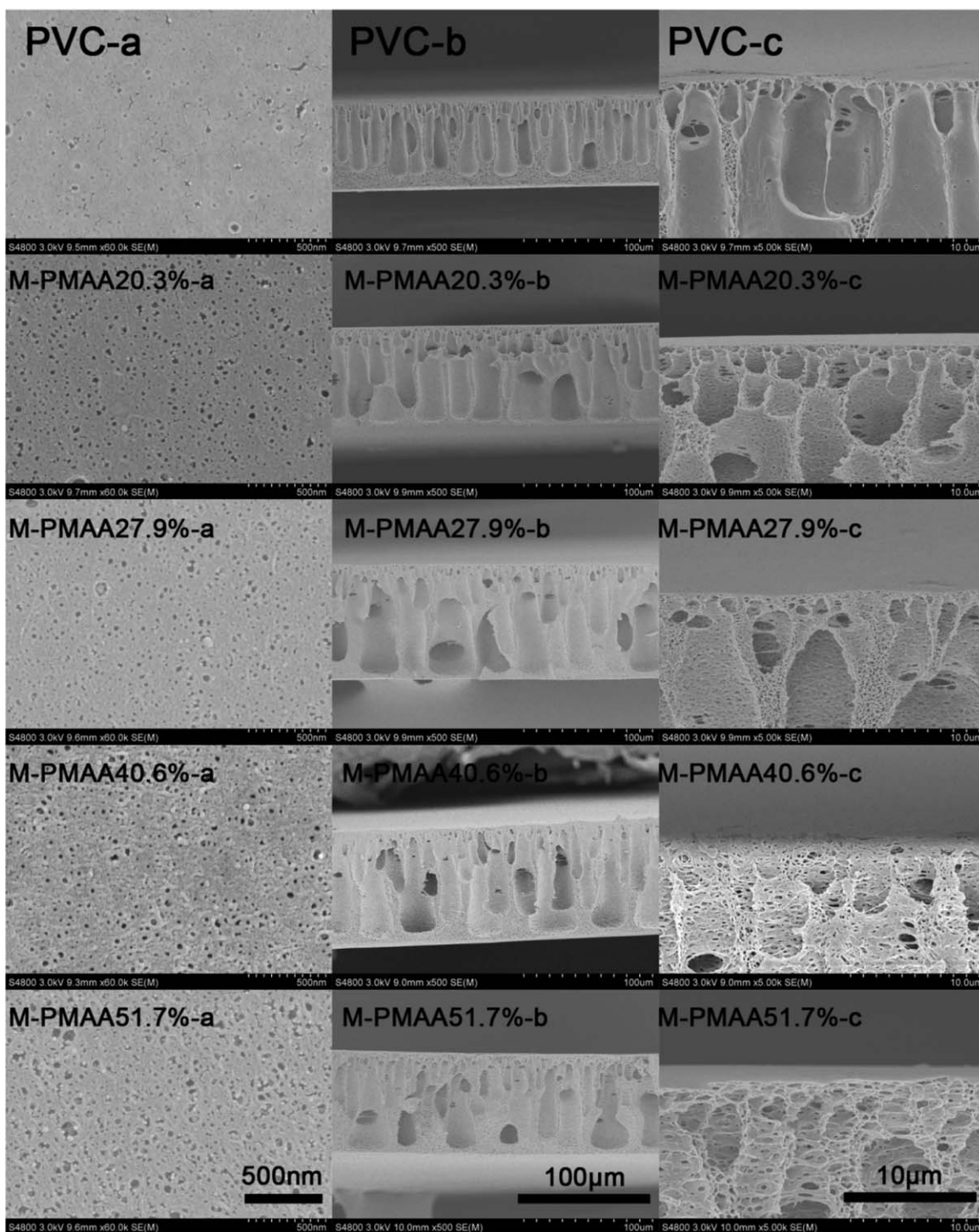
Figure 4. SEM images of PVC and PVC/PVC-*g*-PMAA blend membranes (a: top surface; b: cross section; c: magnified cross section).

Figure 3(d) displays surface zeta potential plotted against the pH of PVC and PVC/PVC-*g*-PMAA membranes. Due to the introduction of PMAA into PVC blend membranes, the surface charge of blend membranes changes significantly. Compared to PVC curve, all zeta potential plots of blend membranes shift towards the lower zeta potential. The isoelectric point for PVC membrane is 5.5 and those for M-PMAA20.3, M-PMAA27.9, M-PMAA40.6, and M-PMAA51.7% are 4.7, 4.1, 3.6, and 3.4,

respectively. At pH 7.0, the negative charge decreases with the increase of PMAA content in the copolymer. This phenomenon is ascribed to the existence of PMAA chains in the blend membrane. Since the *pKa* of PMAA is about 5–6, the carboxylic acid groups exist in the form of COOH when pH is lower than 5, whereas the carboxylic acid groups are deprotonated when pH is over 6. Therefore, when pH is 7.0, all carboxylic acid groups in blend membranes convert into COO^-, resulting in negative charge on

Table IV. Porosities of PVC and PVC/PVC-*g*-PMAA Blend Membranes

Membrane ID	PVC	M-PMAA20.3%	M-PMAA27.9%	M-PMAA40.6%	M-PMAA51.7%
Porosities (*P* %)	64.1 ± 5.1	76.4 ± 2.9	77.4 ± 1.6	78.0 ± 0.6	78.8 ± 3.0

the surface. In addition, the increasing COOH concentration on the surface further raise the surface charge on the blend membranes.

Surface wettability was determined by the water contact angle on the surfaces. Generally, higher contact angle represents the hydrophobicity of the membrane, whereas lower contact angle means the more hydrophilic surface. Figure 3(e) displays the static contact angles of PVC and PVC/PVC-*g*-PMAA blend membranes. As it can be seen, the contact angle for PVC membrane is high with a value of 89.4° indicating the intrinsic hydrophobicity of PVC. However, the contact angles of blend membranes drop obviously and they are even lower than 60°. This enhanced wettability is due to the hydrogen bonding between PMAA chains and water, which improves the interaction between blend membranes and water. In addition the COOH groups are partially ionized in water and exist in the form of COO^-, which also would improve the water binding capacity of PMAA chains as well as the hydrophilicity of blend membranes. Furthermore, the COOH concentration on the surface increases with the increase of PMAA grafting degree. This promotes the decrease in contact angles, which would be beneficial for the permeability and antifouling properties of blend membranes.

The morphologies of PVC and PVC/PVC-*g*-PMAA blend membranes were visualized by SEM (Figure 4). All membranes display an asymmetrical structure with dense top layer and finger-like pores in the cross section. It can also be seen that the porosity and pore sizes on the top surface increase depending on PVC-*g*-PMAA. However, the blend membrane shows sufficiently developed finger-like pores in the cross section compared to the pure membrane. Also, it could be observed from the magnified cross sectional images of membranes (the right column), that there are almost no pores on the walls of finger-like structures of PVC pure membrane. While in the blend membranes, the pores appear on the wall of macrovoids. The porosities and sizes of these pores increase with the increase of PMAA grafting degree. This phenomenon is familiar with PVC blend membranes as reported in literature.[3,21,35] Due to the hydrophilicity of PMAA chains in copolymers, the interaction between casting solution and coagulation bath is enhanced, which causes more coagulation bath to enter the casting solution. This leads to the formation of large size polymer-lean region during liquid–liquid demixing, which in turn results in larger pores in the cross section.[36] In addition, since PVC-*g*-PMAA acts as the pore forming agent, the large molecular weight of the additive would lead to larger pore size in both the cross section and on the surface.[37,38] The porosities of PVC and blend membranes were also characterized and shown in Table IV. It can be clearly seen that the porosities of the blend membranes increase rapidly when blending with PVC-*g*-PMAA. The porosities of the blend membranes increase from 76.4 to 78.8%,

when PMAA grafting degree is increased from 20.3 to 51.7%, indicating a suppression in growth rate. All these results are in accordance with the SEM observation.

Figure 5 shows the permeability and separation performance of PVC and blend membranes, where BSA is used as the model solute. It can be seen that the water flux and BSA rejection for PVC pure membrane is 21.4 L m^{-2} h^{-1} and 98.4%, respectively. The fluxes for blend membranes initially increase and then decreases with the increasing PMAA grafting degree, whereas BSA rejections decrease at first and then increases. The flux for M-PMAA27.9% being 87.0 L m^{-2} h^{-1} is the largest among all the membranes. The reason could be interpreted as follows. First, PVC-*g*-PMAA plays the role of hydrophilic additive which would improve the wettability of blend membrane and helps water to permeate into the membrane. Secondly, it acts as the pore forming agent, which increases the surface pores and porosity creating more easy ways for water permeation. Combining these two factors, the permeability of the blend membrane is obviously elevated. However, when too much PMAA chains are incorporated into PVC matrix, the water permeability is suppressed, which in turn is responsible for the large 'dragging' effect exerted by the longer hydrophilic PMAA graft chains at the solid–liquid interface.[27,39] As for the separation performance is concerned, the pore forming effect of amphiphilic copolymer enlarges the surface pores of blend membranes, which causes a decreased BSA rejection. On the other hand, enhanced negative charge on the surface would retrain the permeation of solute with negative charges to some extent due to the electrostatic repulsion, inducing a small increase in BSA rejection. Due to the above reasons, the blend membrane with PMAA27.9% exhibits the largest flux and a good separation performance.

To compare the antifouling property of PVC pure and blend membranes, protein solution adsorption and filtration
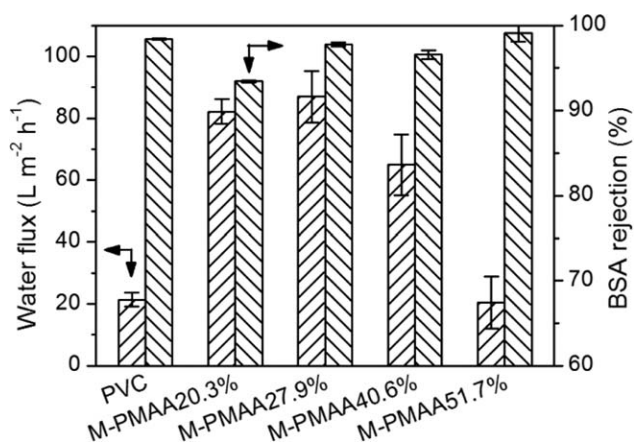
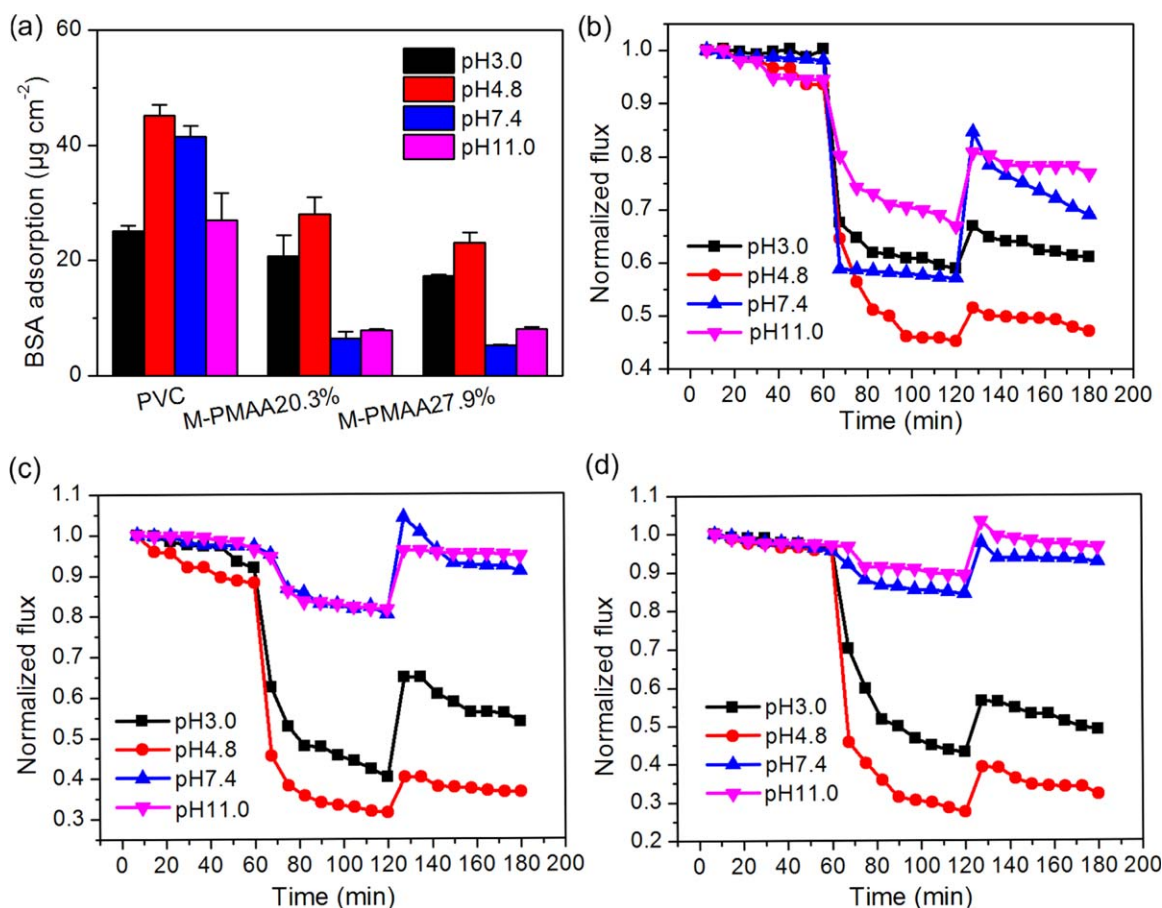**Figure 5.** Water fluxes and BSA rejections of PVC and PVC/PVC-*g*-PMAA blend membranes.

Figure 6. (a) BSA adsorption for PVC and PVC/PVC-*g*-PMAA blend (M-PMAA20.3 and M-PMAA27.9%) membranes in BSA (0.5 g L^{-1}) solution with different pH (3.0, 4.8, 7.4, and 11.0); the time-dependent normalized fluxes for (b) PVC pure membrane and PVC/PVC-*g*-PMAA blend membranes ((c) M-PMAA20.3% and (d) M-PMAA27.9%) at different pH (3.0, 4.8, 7.4, and 11.0) during the process of BSA filtration (0–60 min PBS flux, 60–120 min BSA solution flux, 120–180 min PBS flux). The rinsing process for about 30 min is not included in the diagram. [Color figure can be viewed in the online issue, which is available at wileyonlinelibrary.com.]

experiment were carried out. Owing to the different forms of PMAA chains in different pH environment, the antifouling ability at different pH was carefully investigated. Figure 6(a) shows the protein adsorption for PVC and PVC/PVC-*g*-PMAA blend membranes at different pH. BSA, whose isoelectric point is 4.8, is used as the model molecule. As can be seen in Figure 6(a), the amount of BSA adsorption on blend membranes is lower than that on PVC membranes at all pH range and the amount increases initially, but then decreases with the increasing pH. When pH is equal to the isoelectric point of BSA, protein molecules become uncharged. The intermolecular interaction as well as the interaction between the membrane and BSA molecules are weak, which results in the aggregation and deposition of proteins on the surfaces. When pH is 3.0, the same charge on the membrane surface and BSA molecules as well as the improved hydrophilicity causes a slight decrease in BSA adsorption such that the amount of BSA protein adsorption on the blend membranes is 20 μg cm^{-2}. But when pH is 7.4 or 11.0, the grafting PMAA chains are endowed with negative charge which is the same with that of protein molecules and strong electrostatic repulsion would retard the contact of BSA and the surface. Moreover, the segregated hydrophilic chains would help

to form an ultrathin hydrated layer to avoid the proteins to touch the hydrophobic matrix. Both factors lead to the reduction of BSA adsorption remarkably.[40] Therefore, the introduction of amphiphilic copolymer PVC-*g*-PMAA into PVC membranes effectively improve the resistance towards BSA adsorption, especially when pH is 7.4 or 11.0.

To further research the antifouling ability of blend membranes, a dynamic protein solution filtration experiment at different pH was conducted and the results are shown in Figure 6(b–d). During the BSA filtration process, the foulants adsorb or deposit or even form a filter cake on the surfaces as well as the pores of membranes. This would reduce the pore size on the surfaces and even block the tunnels for water permeation, which causes a reduction in membrane permeability. During the rinsing process, the adsorbed foulants could be partially washed away and the flux would recover to some degree.

As can be seen in Figure 6(b–d), the BSA fluxes of all the membranes decline drastically when pH is 4.8. As discussed above, BSA tends to adhere and deposit on the surface and pores of membranes resulting in the lowest BSA fluxes. For the same reasons, the membranes at pH 4.8 show the lowest flux recovery
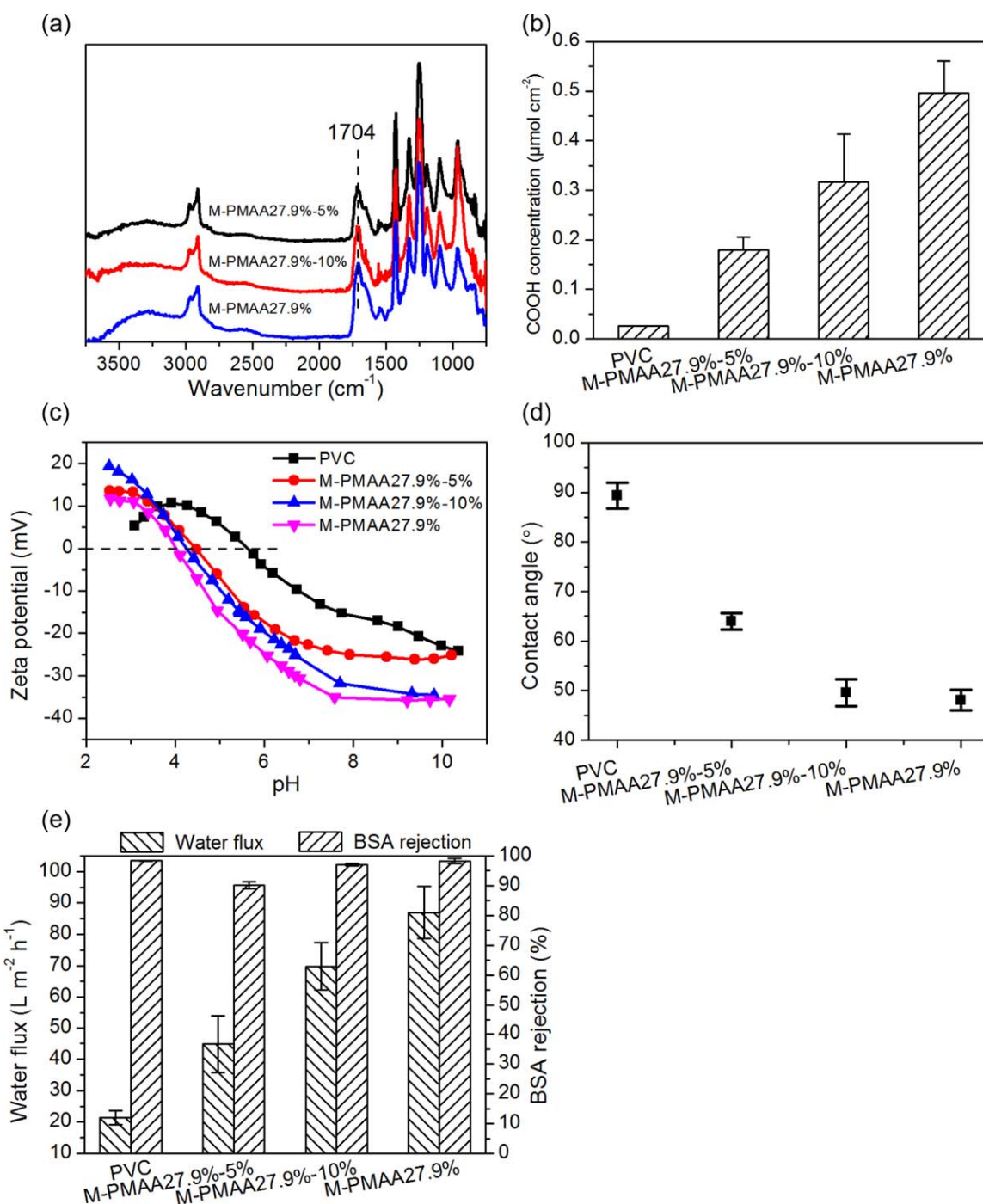
Figure 7. (a) ATR-FTIR spectra, (b) surface COOH concentration, (c) zeta potential plotted against pH, (d) the static contact angles, (e) the water flux and BSA rejection of PVC, and PVC/PVC-g-PMAA blend (M-PMAA27.9–5, M-PMAA27.9–10, and M-PMAA27.9%) membranes. [Color figure can be viewed in the online issue, which is available at wileyonlinelibrary.com.]

ratio (FRR, FRR = J_{w2}/J_{w1}) (Supporting Information Table SI) in all the pH range. It is well known that FRR values could quantitatively describe the antifouling ability during membrane filtration[35] such that the higher values represent the better fouling resistance. This indicates that the membranes exhibit the worst antifouling ability at pH 4.8. Because of the hydrophobic nature of PVC membranes, FRR at different pH are relatively low, which indicates the bad fouling resistance of the pure

membrane. But for the blend membranes, FRR is obviously raised from 0.94 to 0.99 when the pH is 7.4 or 11.0. This phenomenon can be explained as follows. On one hand, the blend membranes are endowed with negative charge which would repel the negative protein molecules. On the other hand, the hydrophilicity is significantly improved due to the presence of hydrophilic COO^- groups. The formed hydrated layer would reduce the contact between proteins and membranes. However,
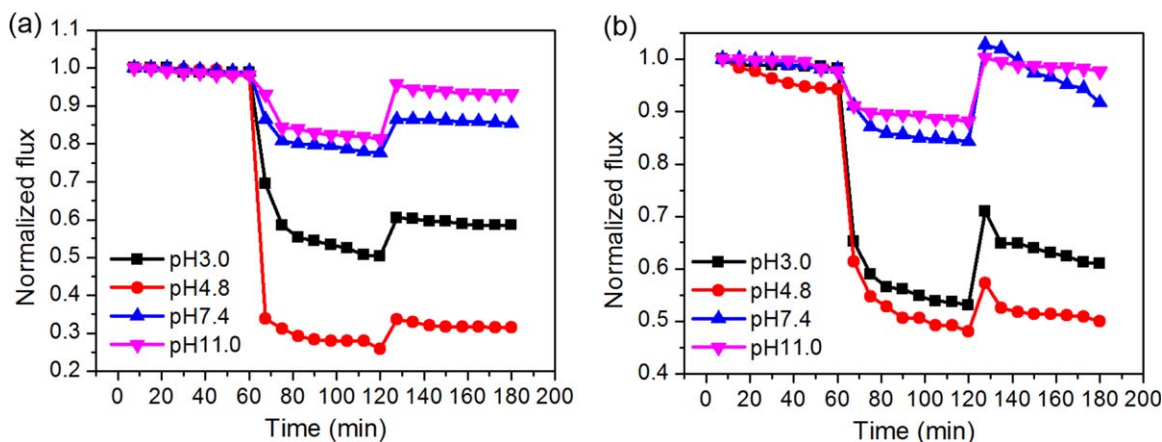
Figure 8. Time-dependent fluxes for PVC/PVC-*g*-PMAA blend membranes (a: M-PMAA27.9–5%, b: M-PMAA27.9–10%) at different pH (3.0, 4.8, 7.4, and 11.0) during the process of BSA filtration. [Color figure can be viewed in the online issue, which is available at wileyonlinelibrary.com.]

when pH is 3.0, FRR for blend membranes is relatively low indicating a bad fouling resistance at this condition. It may be caused by the BSA adsorption on the surfaces as discussed above.

Generally, membrane fouling could be divided into reversible fouling and irreversible fouling. Total fouling ($R_t = (J_{w1} - J_p)/J_{w1}$), reversible fouling ($R_r = (J_{w2} - J_p)/J_{w1}$), irreversible fouling ($R_{ir} = (J_{w1} - J_{w2})/J_{w1}$), relative reversible fouling (RRF = R_r/R_t) and relative irreversible fouling (RIF = R_{ir}/R_t) are calculated and presented in Supporting Information Table SI. Since the membranes are mainly used in neutral condition, the membrane fouling at pH 7.4 is extensively discussed. Compared to PVC membrane, R_t of blend membranes decreases significantly and RIF of the blend membranes is much lower than that of PVC membrane. Moreover, with the increase of PMAA grafting degree in PVC/PVC-*g*-PMAA blend membrane, R_t and RIF decrease consequently. These phenomena could be interpreted that the irreversible fouling is restrained by the introduction of PVC-*g*-PMAA. The improved hydrophilicity of the blend membranes would reduce the adsorption and deposition of proteins on their surface, leading to the suppressed membrane fouling. Moreover, the attached foulants on the hydrophilic surfaces can be eliminated more easily by hydraulic cleaning, suggesting a reduced irreversible fouling. In summary, due to the incorporation of PVC-*g*-PMAA into PVC membranes, the antifouling ability of blend membranes is significantly improved especially at neutral or alkaline environments.

Effect of PVC-*g*-PMAA Concentration on the Structures and Performances of the Blend Membranes

In order to investigate the effect of PVC-*g*-PMAA concentration in the PVC/PVC-*g*-PMAA membranes, the blend membranes with different concentration of PVC-*g*-PMAA were prepared and the structures as well as their performances were analyzed. It can be seen in Figure 7(a), the strong adsorption peak at 1704 cm^{-1} appears in blend membranes and the intensity of the peak increases with the PVC-*g*-PMAA concentration. This means that the surface PMAA chains increase when the concentration is increased from 5 to 20%. The observed surface chemical compositions shows a dependency with the surface COOH

concentrations [Figure 7(b)], which are 0.18, 0.31, and 0.50 μmol cm^{-2} for M-PMAA27.9–5, M-PMAA27.9–10, and M-PMAA27.9%, respectively. Accordingly, the values of surface charge and water contact angle on the surfaces of blend membranes are reduced with the increase in PVC-*g*-PMAA concentration [Figure 7(c,d)]. The reason is the same as explained in section "Effect of PMAA Grafting Degree in PVC-*g*-PMAA on the Structures and Performances of the Membranes"; that is, the increasing COOH concentration would produce more COO$^-$ groups, which represents the lower surface charge. Meanwhile, the higher COOH concentration would enhance the water binding capability of blend membranes, which helps water to spread and diffuse on to/into the surface, resulting in better hydrophilicity. Due to the pore forming nature of PVC-*g*-PMAA, the surface pore sizes, the size of macrovoids in the cross section, the pore sizes on the finger-like structure and the porosities of the blend membrane increase with the PVC-*g*-PMAA concentration (Supporting Information Figure SII and Table SII). Hence, due to the improved hydrophilicity and pore structures, the permeability of the membrane increases gradually [Figure 7(e)]. However, there is only a little increase in BSA rejection of the membrane, which is mainly ascribed to the electrostatic repulsion of the same charge on the membrane surface and protein molecules. The blend membrane shows the best performance when the PVC-*g*-PMAA content is 20%.

In addition, the antifouling ability of the blend membranes with different PVC-*g*-PMAA concentration was also evaluated by protein solution filtration experiment. The time dependent fluxes for PVC/PVC-*g*-PMAA blend membranes at different pH are shown in Figure 8 and the types of the membrane fouling are presented in Supporting Information Table SI and SIII. The values of FRR for PVC/PVC-*g*-PMAA blend membranes are much higher than that of PVC pure membrane at pH 7.4 and they are 0.70, 0.86, 0.94, and 0.97 for PVC, M-PMAA27.9–5, M-PMAA27.9–10, and M-PMAA27.9%, respectively. A similar increasing order of FRR is also observed when the pH is 11.0. The value of *FRR* is found to gradually increase with the PVC-*g*-PMAA concentration, which indicates that the antifouling ability of the blend membrane gradually improves on increasing

PVC-*g*-PMAA content in the membrane. On the other hand, the total fouling (R_t) and relative irreversible fouling (RIF) decrease from 0.42 to 0.12 and from 0.71 to 0.26, respectively, implying a reduced irreversible fouling. Therefore, the increase in PVC-*g*-PMAA concentration effectively enhances the antifouling ability, especially to reduce irreversible fouling.

CONCLUSIONS

In this study, amphiphilic copolymer PVC-*g*-PMAA was synthesized by ATRP method followed by a hydrolysis reaction. The PMAA grafting degree in the copolymer could be regulated by adjusting ATRP reaction time. The PVC/PVC-*g*-PMAA blend membranes were prepared via NIPS process and PVC-*g*-PMAA was found to be segregated towards the membrane surface. Due to the deprotonation ability of PMAA chains, the blend membranes were endowed with negative charge and an improved hydrophilicity. The blend membrane exhibited the largest flux and a good separation performance, when the concentration of PMAA27.9% was 20 wt %. Due to the existence of PMAA chains in the copolymer, the blend membranes showed a better protein adsorption resistance and antifouling ability especially at neutral or alkaline environments.

ACKNOWLEDGMENTS

REFERENCES

1. Rana, D.; Matsuura, T. *Chem. Rev.* **2010**, *110*, 2448.

2. Chapman, J.; Lawlor, A.; Weir, E.; Quilty, B.; Regan, F. *J. Membr. Sci.* **2010**, *365*, 180.

3. Liu, B.; Chen, C.; Zhang, W.; Crittenden, J.; Chen, Y. *Desalination* **2012**, *307*, 26.

4. Zhu, L.; Zhu, L.; Zhao, Y.; Zhu, B.; Xu, Y. *J. Mater. Chem. A* **2014**, *2*, 15566.

5. Sui, Y.; Wang, Z.; Gao, X.; Gao, C. *J. Membr. Sci.* **2012**, *413*, 38.

6. Hester, J. F.; Banerjee, P.; Mayes, A. M. *Macromolecules* **1999**, *32*, 1643.

7. Rajabzadeh, S.; Sano, R.; Ishigami, T.; Kakihana, Y.; Ohmukai, Y.; Matsuyama, H. *Appl. Surf. Sci.* **2014**, *324*, 718.

8. Liu, L.; Chen, H.; Yang, F. *Sep. Purif. Technol.* **2014**, *133*, 22.

9. Kumar, M.; Ulbricht, M. *Sep. Purif. Technol.* **2014**, *127*, 181.

10. Saffar, A.; Carreau, P. J.; Ajji, A.; Kamal, M. R. *J. Membr. Sci.* **2014**, *462*, 50.

11. Hidzir, N. M.; Hill, D. J. T.; Martin, D.; Grondahl, L. *Polymer* **2012**, *53*, 6063.

12. Hester, J. F.; Mayes, A. M. *J. Membr. Sci.* **2002**, *202*, 119.

13. Hester, J. F.; Banerjee, P.; Won, Y. Y.; Akthakul, A.; Acar, M. H.; Mayes, A. M. *Macromolecules* **2002**, *35*, 7652.

14. Taniguchi, M.; Kilduff, J. E.; Belfort, G. *J. Membr. Sci.* **2003**, *222*, 59.

15. Yu, H.-Y.; Xu, Z.-K.; Yang, Q.; Hu, M.-X.; Wang, S.-Y. *J. Membr. Sci.* **2006**, *281*, 658.

16. Liang, S.; Kang, Y.; Tiraferri, A.; Giannelis, E. P.; Huang, X.; Elimelech, M. *ACS Appl. Mater. Interfaces* **2013**, *5*, 6694.

17. Hester, J. F.; Olugebefola, S. C.; Mayes, A. M. *J. Membr. Sci.* **2002**, *208*, 375.

18. Muth, O.; Hirth, T.; Vogel, H. *J. Supercrit. Fluids* **2000**, *17*, 65.

19. Liu, P.; Zhang, L. *J. Macromol. Sci. Pure Appl. Chem.* **2007**, *45*, 17.

20. Liu, P.; Liu, Y.; Su, Z. *Ind. Eng. Chem. Res.* **2006**, *45*, 2255.

21. Liu, W.; Zhang, Y.; Fang, L.; Zhu, L. *Chin. J. Polym. Sci.* **2012**, *30*, 568.

22. Bicak, N.; Ozlem, M. *J. Polym. Sci. A: Polym. Chem.* **2003**, *41*, 3457.

23. Percec, V.; Asgarzadeh, F. *J. Polym. Sci. A: Polym. Chem.* **2001**, *39*, 1120.

24. Bicak, N.; Karagoz, B.; Emre, D. *J. Polym. Sci. Part A: Polym. Chem.* **2006**, *44*, 1900.

25. Oh, J. H.; Chi, W. S.; Lee, J. H.; Kim, J. H.; Kang, S. W. *Ind. Eng. Chem. Res.* **2013**, *52*, 9607.

26. Zhang, R.; Su, Y.; Peng, J.; Fan, X.; Jiang, Z.; Zhao, X.; Liu, J.; Li, Y.; Zhao, J. *Polymer* **2014**, *55*, 1347.

27. Luo, T.; Lin, S.; Xie, R.; Ju, X.; Liu, Z.; Wang, W.; Mou, C.; Zhao, C.; Chen, Q.; Chu, L. *J. Membr. Sci.* **2014**, *450*, 162.

28. Ying, L.; Yin, C.; Zhuo, R.; Leong, K.; Mao, H.; Kang, E.; Neoh, K. *Biomacromolecules* **2003**, *4*, 157.

29. Kang, E.; Tan, K.; Kato, K.; Uyama, Y.; Ikada, Y. *Macromolecules* **1996**, *29*, 6872.

30. Möckel, D.; Staude, E.; Dal-Cin, M.; Darcovich, K.; Guiver, M. *J. Membr. Sci.* **1998**, *145*, 211.

31. Xie, H.; Saito, T.; Hickner, M. A. *Langmuir* **2011**, *27*, 4721.

32. de Groot, G. W.; Santonicola, M. G.; Sugihara, K.; Zambelli, T.; Reimhult, E.; Voeroes, J.; Vancso, G. *J. ACS Appl. Mater. Interfaces* **2013**, *5*, 1400.

33. Schmitz, C.; Mourran, A.; Keul, H.; Möller, M. *Macromol. Chem. Phys.* **2008**, *209*, 1859.

34. Zhu, L.; Xu, L.; Zhu, B.; Feng, Y.; Xu, Y. *J. Membr. Sci.* **2007**, *294*, 196.

35. Fan, X.; Su, Y.; Zhao, X.; Li, Y.; Zhang, R.; Zhao, J.; Jiang, Z.; Zhu, J.; Ma, Y.; Liu, Y. *J. Membr. Sci.* **2014**, *464*, 100.

36. Zhao, Y.; Zhu, B.; Kong, L.; Xu, Y. *Langmuir* **2007**, *23*, 5779.

37. Wongchitphimon, S.; Wang, R.; Jiraratananon, R.; Shi, L.; Loh, C. H. *J. Membr. Sci.* **2011**, *369*, 329.

38. Xu, J.; Xu, Z.-L. *J. Membr. Sci.* **2002**, *208*, 203.

39. Ying, L.; Wang, P.; Kang, E. T.; Neoh, K. G. *Macromolecules* **2002**, *35*, 673.

40. Boributh, S.; Chanachai, A.; Jiraratananon, R. *J. Membr. Sci.* **2009**, *342*, 97.